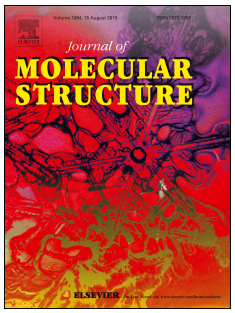

Spectroscopic studies on the potassium 1-fluorobenzoyltrifluoroborate salt by using the FT-IR, Raman and UV–Visible spectra and DFT calculations

Maximiliano A. Iramain, Ana E. Ledesma, Elizabeth Imbarack, Patricio Leyton Bongiorno, Silvia Antonia Brandán

PII: S0022-2860(19)31643-6

DOI: https://doi.org/10.1016/j.molstruc.2019.127534

Reference: MOLSTR 127534

To appear in: *Journal of Molecular Structure*

Received Date: 16 October 2019

Revised Date: 2 December 2019

Accepted Date: 3 December 2019

Please cite this article as: M.A. Iramain, A.E. Ledesma, E. Imbarack, P.L. Bongiorno, S.A. Brandán, Spectroscopic studies on the potassium 1-fluorobenzoyltrifluoroborate salt by using the FT-IR, Raman and UV–Visible spectra and DFT calculations, *Journal of Molecular Structure* (2020), doi: https://doi.org/10.1016/j.molstruc.2019.127534.

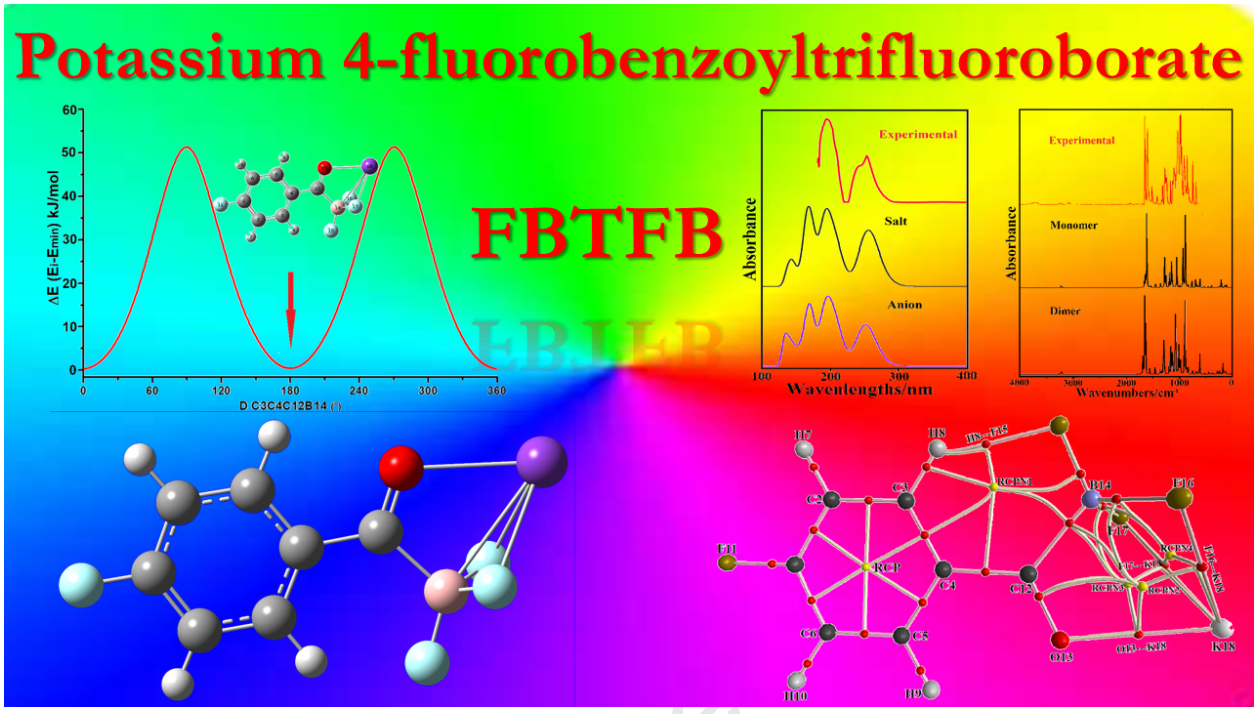

Spectroscopic studies on the potassium 1-fluorobenzoyltrifluoroborate salt by using the FT-IR, Raman and UV-Visible spectra and DFT calculations

Maximiliano A. Iramain[a], Ana E. Ledesma[b], Elizabeth Imbarack[c], Patricio Leyton Bongiorno[c], Silvia Antonia Brandán[a,*]

[a]*Cátedra de Química General, Instituto de Química Inorgánica, Facultad de Bioquímica, Química y Farmacia, Universidad Nacional de Tucumán, Ayacucho 471, 4000, Tucumán, Argentina.*
[b]*Departamento Académico de Química, FCEyT, CIBAAL-UNSE-CONICET, Av. Belgrano Sur 1912, (4200) Santiago del Estero, Argentina.*
[c]*Laboratorio de Fotofísica y Espectroscopia Molecular Nº401, Av. Universidad #330, Campus Curauma, Valparaíso, Pontificia Universidad Católica de Valparaíso, Chile.*

Abstract

Potassium 1-fluorobenzoyltrifluoroborate (FBTFB) salt was characterized using Fourier Transformed Infrared (FT-IR) and Raman solid-state spectroscopies as well as ultraviolet-visible spectroscopy in aqueous solution. The functional hybrid B3LYP with the 6-311++G** basis set have optimized the structures of salt in gas phase and in aqueous solution with C_S symmetries. In solution, the influence of solvent was studied at the same level of theory with the integral equation formalism variant polarised continuum method (IEFPCM) and the universal solvation model. FBTFB has evidenced the lower solvation energy (-81.54 kJ/mol), as compared with other trifluoroborate salts probably due to the presence of F in the 1st position of phenyl ring that decreases the solubility of this salt. NBO studies clearly support the ionic characteristics of K^+F^- and K^+O^- bonds and the high energy values of *LPF17→ LP*B14* transitions ($\Delta E_{n\rightarrow n^*}$) while AIM analyses suggest a high stability of salt in both media due to three ionic and one C-H···F interactions. Analyses of frontier orbitals have suggested that the FBTFB salt is more reactive in solution than in gas phase and, than 2-phenylacetyl-trifluoroborate (PTFB) in the two media possibly because FBTFB presents higher global electrophilicity (ω) and nucleophilicity indexes (E) in both media than PTFB. Here, the calculated harmonic force fields, scaled force constants and complete assignments of all vibration normal modes expected for FBTFB in both media are reported. Predicted IR, Raman and UV-Visible spectra have shown good concordance when they are compared with the corresponding experimental ones.

Keywords: Potassium 1-fluorobenzoyltrifluoroborate salt, vibrational spectra, molecular structure, force field, DFT calculations.

* Corresponding author. Tel.: +54-381-4247752; fax: +54-381-4248169;

E- mail: sbrandan@fbqf.unt.edu.ar (S.A. Brandán)

1. Introduction

Trifluoroborate salts are compounds with fascinating properties in different media evidencing interesting correlations in the common geometrical parameters to BF_3K group and where the halogen H···F interactions have influence on their reactivities and properties [1-7]. The different groups linked to BF_3K group also have impact on their properties, as suggested by the different studies reported in the literature. Hence, when the 2-isonicotinoyl group is linked to trifluoroborate in 2-isonicotinoyl-trifluoroborate (ITFB) the pyridine ring favours the formation of halogen interaction and a shorter H···F distance is observed, as compared with furyl and phenyl rings [1,7]. Besides, when the Br atom is incorporated to pyridine ring, it increases the reactivity of 5-Br-2-isonicotinoyltrifluoroborate (Br-ITFB) salt. Hence, higher solvation energies in aqueous solution are observed for Br-ITFB, 6-chloro-2-isonicotinoyl-trifluoroborate (Cl-ITFB) and IFTB salts, evidencing a certain dependence of solvation energies on the reactivities of these salts [4,5]. Taking into account the importance of position when the halogen is incorporated in the ring and how it affects its structure and the properties of salt, in this work, we have studied the effect of F halogen on the structural, electronic, topological and vibrational properties of potassium 1-fluorobenzoyltrifluoroborate (FBTFB) salt. So far, those properties for FBTFB were not reported yet. The methodology employed in this case is similar to those reported for other salts [1-7]. The combination of functional hybrid B3LYP with the 6-311++G** basis set [8,9] and with the experimental infrared and Raman spectra is useful to perform the complete assignments of bands observed in order to identify the salt in all possible media. As in above studies, the dimeric species of salt and its anion were also considered in this study because some bands observed in the vibrational spectra justify the presence of dimer while in solution the anion is also observed. In aqueous solution, the solvent effect was studied with the integral equation formalism variant polarised continuum method (IEFPCM) while the universal solvation model was employed to calculate the solvation energy at the same level of theory [10-12]. Hence, the scaled quantum mechanical force field (SQMFF) approach and the Molvib program were used with the support of the normal internal coordinates and transferable scaling factors [13-15]. Here, the ultraviolet-visible spectrum in aqueous solution was also reported and the observed bands were also assigned with the aid of time-dependent DFT calculations (TD-DFT) [16]. Reactivities and behaviours of salt in gas phase and aqueous solution were also predicted and compared with the reported for similar salts [1-7]. The study was completed with natural bond orbital (NBO) and atoms in molecules (AIM) calculations in order to calculate atomic charges, stabilization energies, solvation energies and molecular electrostatic potentials [17-19]. Finally, all obtained parameters for this salt were first compared in both media

and, then, with the reported for trifluoroborate salts in order to analyse the effect of incorporation of F in the 1st position of ring (or substitution in position 1 of the ring) and on the properties of salt [1-7].

2. Experimental

The FT-IR spectrum of potassium 1-fluorobenzoyltrifluoroborate (FBTFB) salt in the solid phase has been recorded as KBr pellet in the 4000-400 cm^{-1} region by using a JASCO FTIR-4600 spectrometer equipped with a DLATGS detector (deuterated L-alanine doped triglycine sulfate) with Peltier temperature control. The spectral resolution was 4 cm^{-1} and 16 scans were performed.

Raman spectra were obtained using a Witec Alpha 300 confocal Raman microscope system equipped using an excitation laser wavelength of 785 nm and an electrically cooled CCD camera. The signal was calibrated using the 520 cm^{-1} line of a Si wafer and a 20x objective. The laser power on the samples was 2 mW. The resolution was set to 4 cm^{-1} and 10 scans with an integration time of 1 second were performed. These spectra were recorded over the 200-1800 cm^{-1} region**.**

Beckman spectrophotometer was used to record the electronic spectrum of FBTFB in aqueous solution between 180 and 800 nm. For this salt the region was different to the reported for other salts [1-4,7].

3. Computational details

FBTFB salt was modelled with the *GaussView* program [22] and, later optimized in gas phase and aqueous solution with the Revision A.02 of Gaussian 09 program [18] by using the functional hybrid B3LYP with the 6-311++G** basis set [8,9]. The potential energy surface (PES) was studied to variations in the dihedral C3-C4-C12-B14 angle by using the hybrid B3LYP/6-31G* method due to low computational cost employed in relation to higher size basis set. Thus, the PES for FBTFB is shown in **Figure 1**. The dimeric species of salt and its anion were also optimized at the same level of theory, for which, in **Figure 2** is presented the monomer while in **Figure 3** is shown the dimer together with the anion. The salt was optimized with C_S symmetry in both media. The final energy of dimeric species was corrected by the basis set superposition error (BSSE) [23]. Atomic charges, molecular electrostatic potentials, bond orders, donor-acceptor energy interactions and the topological properties for salt were predicted at the same level of theory by using Gaussian NBO Version 3.1 and AIM2000 calculations [19-21]. The SQMFF methodology and the Molvib program Version 7.0 were employed to perform the vibrational analysis with the aid of normal internal coordinates and transferable scaling factors [15-17]. The electronic spectrum of salt and its anion were predicted in aqueous solution by using the functional hybrid B3LYP and the same basis set with the time-dependent DFT calculations (TD-DFT) [18]. Additionally, reactivities and behaviours of salt were predicted by using calculations of frontier orbitals and the chemical potential (μ),

electronegativity (χ), global hardness (η), global softness (S), global electrophilicity index (ω) and nucleophilicity indexes (E) descriptors [1-7,24-32]. Properties predicted for this salt were compared with those reported for similar salts in order to evaluate the effect of incorporating F in the 1st position on the properties of salt [1-7].

4. Results and discussion

4.1. Geometries of salt in both media

Previous theoretical calculations performed with the functional hybrid B3LYP and the 6-311++G** basis set for other trifluoroborate salts have evidenced different symmetries after they were optimized in different media, thus, the potassium 3-furoyl-trifluoroborate (FTFB), 2-isonicotinoyl-trifluoroborate (ITFB), 6-chloro-2-isonicotinoyl-trifluoroborate (Cl-ITFB) and 4-fluorobenzoyl-trifluoroborate (FBTFB) salts have shown C_S symmetries in both media, with exception of Cl-ITFB that change from C_S in gas phase to C_1 in solution while the 5-hydroxypentanoyl-trifluoroborate (HTFB), 5-Br-2-isonicotinoyl-trifluoroborate (Br-ITFB) and 2-phenylacetyl-trifluoroborate (PTFB) salts clearly evidence C_1 symmetries in both media [1-7]. Evidently, the Cl halogen in the pyridine ring of Cl-ITFB salt generates different behaviour in solution. Here, the structures of FBTFB salt in both media have been optimized with C_S symmetries, as in the cases of FTFB and ITFB salts. In Table 1, the total energy corrected by ZPVE, moment dipolar, volume and solvation energy values of FBTFB are observed in both media by using the functional hybrid B3LYP with the 6-311++G** basis set. The Cartesian coordinates of all atoms of optimized structures in both media are summarized in **Table S1**. The Moldraw program was used to calculate the volume values of salt in both media [33]. As expected, the dipole moment value increases in solution because its anion is present in this medium quickly evidencing its hydration by the increase in the volume. Comparisons of properties of trifluoroborate salts in both media at the same level of theory are presented in **Table 2** together with the molecular weights (MW) for each salt while in **Figure 4** the volume variations and the dipole moment values are shown in both media as functions of their molecular weights. Fig 4a clearly shows that the volume variations decrease with the increase of MW, having the ITFB salt higher variation while the presence of halogen in the salt notably reduces the difference between the volume in solution and the volume in gas phase. Thus, the Br-ITFB presents the lowest volume variation. The dipole moment values evidence practically the same behaviors in both media, as observed in Fig. 4b, showing the higher values HTFB and FBTFB and the lower values the ITFB and Cl-ITFB salts. The former result is in agreement with the absence of halogen H···F bonds in the respective salts [6]. Table 2 shows that the FBTFB salt has lower solvation energy while the HTFB salt reveals the most negative and highest value. The presence of an OH group and the absence of an

aromatic ring clearly justify the higher hydration of this salt and the higher dipole moment value predicted in solution. On the contrary, the presence of F in the 1st position of benzyl ring linked to trifluoroborate group in the FBTFB salt could probably support its low solvation energy (-81.54 kJ/mol).

Comparisons of geometrical parameters calculated for FBTFB in gas phase and aqueous solution by using the functional hybrid B3LYP with the 6-311++G** basis set with the corresponding to the experimental structure 5C determined by X-ray diffraction for Potassium 1-chlorobenzoyltrifluoroborate salt by Dumas and Bode [34] are presented in **Table 3**. So far, the experimental structure of FBTFB was not published and, for this reason, the predicted structures were compared with that reported for the Cl salt by using the root-mean-square deviation (RMSD) values. **Figure S1** shows that the halogen atoms are the only difference between both structures while in **Figure S2** the structures of all trifluoroborate salts previously studied are shown. Hence, when the geometrical parameters predicted for the F salt in both media are deeply analysed, it is observed for bond lengths and angles the same RMSD values in both media where the predicted values in gas phase are similar to the observed in aqueous solution (0.065/0.064 Å and 1.0 º). However, important differences in the C4-C12-B14-F15, C12-B14-F16-K18 and C4-C12-B14-F16 dihedral angles are clearly observed in both media, in relation to the experimental ones. Experimentally, in the Cl salt the C4-C12-B14-F15 dihedral angle has a value of -46.3 º, however, these angles in the F salt in both media are predicted with value null. On the other hand, the calculations predicted the C12-B14-F16-K18 dihedral angle in both media between 71.6 and 72.6 º but in Cl salt has a value of 120.6 º. The C4-C12-B14-F16 dihedral angles in F salt are predicted between 124.4 and 123.5 º while in Cl salt the experimental value observed is 73.0 º. Hence, those three dihedral angles suggest changes in the structure of salt when in the position 1 of ring the Cl atom is changed by F. These differences can simply be seen in the high RMSD values of F salt in both media (47.5/47.2 º). Regarding the good correlations between the structures of both F and Cl salts, especially in the bond lengths and angles, the theoretical structures of F salt predicted in the two media can be used to perform their corresponding vibrational analyses.

4.2. Atomic Charges and bond orders studies

Atomic natural population (NPA) and Mulliken charges and bond orders in trifluoroborate salts are parameters that necessarily should be known due to the presence of strong electropositive (K^+) and electronegative atoms (F^-) in these salts that could justify the presence of different ionic and H bonds interactions [1-7]. Hence, the calculated atomic Mulliken and NPA charges for FBTFB in gas phase and aqueous solution by using B3LYP/6-311++G** level of theory are presented in **Table S2** while in **Figure S3** the behaviours of both charges in gas phase are given. This latter figure perfectly shows

the differences between both charges where clearly the behaviours of the Mulliken charges on all C atoms are different from the NPA charges showing the most positive Mulliken value on the C4 atom and the most negative values on the C3 and C12 atoms. The C3-C12 bond is linked to C=O and to trifluoroborate group. Note that the NPA charge on the C12 atom shows a positive value. Both charges on all H atoms practically present the same values while on the F and O atoms the NPA charges present the most negative values than the Mulliken ones.

Bond orders expressed as Wiberg indexes were also calculated for this salt in both media because the characteristics of different bonds can be easily seen through its values. Thus, in **Table S3** the bond orders (BO) of all atoms of FBTFB are observed in both media together with the matrixes calculated for the most important bonds. Then, Table S2 shows the higher value for the C12-B14 bonds (0.790 in gas phase and 0.813 in solution) while values between 0.705 and 0.588 are observed for the B14-F15, B14-F16 and B14-F17 bonds. On the other hand, the matrix of BO clearly shows the lower values in the K18-O13, K18-F15, K18-F16 and K18-F17 bonds (0.071 and 0.002) because these bonds present ionic characteristics in both media, as in other trifluoroborate salts [1-4].

4.3. NBO and AIM studies

Above studies on atomic charges and bond orders for FBTFB in both media have clearly evidenced different characteristics in the C-B, B-F, K-F and K-O bonds, hence, probably the stability of this salt depends on the nature of those bonds. Thus, from natural bond orbital (NBO) and atom in molecules (AIM) calculations, it is possible to predict the stabilities of this salt in both media by using the functional hybrid B3LYP with the 6-311++G** basis set and the corresponding programs [19-21]. Therefore, in **Table S4** the main delocalization energies for the salt in both media are presented. Six and seven different interactions are observed in gas phase and aqueous solution, respectively. The following interactions are observed in gas phase $\Delta E_{\pi\rightarrow\pi^*}$, $\Delta E_{n\rightarrow\sigma^*}$, $\Delta E_{n\rightarrow\pi^*}$, $\Delta E_{\pi^*\rightarrow\pi^*}$, $\Delta E_{n\rightarrow n^*}$ and $\Delta E_{n^*\rightarrow n^*}$ while the $\Delta E_{\pi^*\rightarrow n^*}$ interaction of very low energy is also observed in solution (71.39 kJ/mol). The most important interactions with high energy values in both media are those observed from lone pairs of F atoms to anti-bonding orbitals of lone pairs of B atom ($\Delta E_{n\rightarrow n^*}$) showing a slightly higher value in solution (5344.44 kJ/mol) than the observed in the gas phase (5358.26 kJ/mol). In this salt, the total energy in gas phase (8503.69 kJ/mol) is higher than the value in aqueous solution (7914.54 kJ/mol); as it was also observed in the 2-phenylacetyl-trifluoroborate (PTFB) salt [7]. Hence, this salt is more stable in gas phase, as compared with the value in solution. Hence, probably the lower stability in aqueous solution could justify the low solvation energy value of FBTFB in this medium (-81.54 kJ/mol) in relation to the values observed for other trifluoroborate salts [1-7].

Other different forms to evaluate the stability of a species is by using the topological properties from the Bader's theory of atoms in molecules because these properties allow to predict possible intra-molecular, H bonds and ionic interactions [20]. This way, the topological properties, such as the electron density, $\rho(r)$, the Laplacian values, $\nabla^2\rho(r)$, the eigenvalues $(\lambda1, \lambda2, \lambda3)$ of the Hessian matrix and the $\lambda1/\lambda3$ ratio in the bond critical points (BCPs) and in the ring critical points (RCPs) were calculated for FBTFB with the AIM2000 program [21]. Then, all those parameters together with the distances between both involved atoms can be seen in **Table S5**. Previously, the $\rho(r)$ and $\nabla^2\rho(r)$ values for similar trifluoroborate salts were already published [6]. Thus, four interactions are observed in both media which are one H bond interaction (C3-H8···F15) and the other three ionic interactions ($K18^+F16^-$, $K18^+F17^-$ and a $K18^+O13^-$) where all these interactions are characterized by a ratio of $\lambda1/\lambda3 < 1$ and $\nabla^2\rho(r) > 0$. Here, the IUPAC notation was used to represent the four interactions observed in FBTFB [35]. Note that the distances between the atoms involved in the interactions increase in solution due to the hydration. In **Figure 5** , the molecular graphic of salt in gas phase showing the four BCPs, the RCP own of 1-fluorobenzoyl ring and the four new RCPs defined as RCPN from 1 up to 4 can be easily seen. These studies suggest that the four different interactions confer a high stability to this salt in both media.

4.4. Frontier orbitals and global descriptors studies

Above studies on trifluoroborate salts [1-7] have evidenced the importance to analyse the frontier orbitals in both media because from its differences, as mentioned by Parr and Pearson, it is possible to predict the reactivities of salts [24]. In addition, the behaviours of these salts also can be predicted calculating common descriptors, such as the chemical potential (χ), electronegativity (μ), hardness (η), softness (S), global electrophilicity index (ω) and global nucleophilicity index (E) [1-7,25-32]. Then, in **Table S6** the frontier orbitals, gap values and the mentioned descriptors for FBTFB in both media together with the corresponding equations used and its comparisons with the parameters calculated for 2-phenylacetyl-trifluoroborate (PTFB) salt [7] are summarized. If first we analyse the gap values for FBTFB in both media, a slight reduction of gap value in solution is observed, indicating that FBTFB is more reactive in this medium than in gas phase while from the comparison with the PTFB salt clearly we observed that FBTFB is more reactive than PTFB in the two media. These comparisons for both salts can visibly be seen in **Figure S4**. Evidently, in PTFB the presence of a CH_2 group between the benzyl ring and the C-BF_3K group produces an increase in its gap value although PTFB is more reactive in gas phase than in solution [7]. When the descriptors for both salts are analysed from **Figure S5**, it is clearly observed that FBTFB presents higher global

electrophilicity (ω) and nucleophilicity indexes (E) in both media than PTF visibly B. Hence, the higher reactivity of FBTFB can be simply attributed to the higher values of those two indexes.

4.5. Vibrational study

Calculations by using the functional hybrid B3LYP with the 6-311++G** basis set have optimized the FBTFB salt in both media with C_S symmetry, as in the FTFB, ITFB and Cl-ITFB salts [1,2] but different from the HTFB, Br-ITFB and PTFB salts which were optimized with C_1 symmetries [3-7]. In **Figures 6** and **7** the experimental FT-IR and Raman spectra of FBTFB salt in the solid state compared are presented with the corresponding predicted for monomer and dimer, respectively. Only, 48 vibration normal modes with activities in both spectra are expected for the monomer of the salt. These modes are classified as 32 A' + 16 A'' where the A' modes are in-plane modes while the A'' are out-of-plane modes. Note that the intensities and the number of bands observed in the IR and Raman spectra of salt in the 1500-1000 cm^{-1} region are clearly justified by its dimeric species, as evidenced in Figures 6 and 7. Otherwise, the presence of dimer generates better correlations in both spectra and, in particular, when the predicted Raman spectra of monomer dimer in activities are transformed to intensities, as observed in **Figure 8** [36]. Harmonic force fields for FBTFB salt in both media were calculated with the SQMFF approach while the experimental IR and Raman spectra were employed to perform the complete assignments in both media considering the internal normal coordinates, potential energy distributions (PED) ≥ 10% and the Molvib program [15-17]. In **Table 4** the experimental and calculated wavenumbers can be seen according to the A' and A'' symmetries together with the assignments for the salt in both media by using the functional hybrid B3LYP with the 6-311++G** basis set. Some assignments are discussed below.

4.5.1. Band Assignments

4.5.1.1. CH modes. For FBTFB in both media, are expected four C-H stretching modes corresponding to phenyl ring which are predicted by the calculations with A' symmetries between 3095 to 3058 cm^{-1}, hence, the very weak bands observed in this region are assigned to these vibration modes, as in similar salts [1-4]. In solution, these modes are predicted at higher wavenumbers than in gas phase. Raman bands in this region are not experimentally observed. In the same way, the C-H rocking modes or in-plane deformation modes are predicted with A' symmetries between 1481 to 1085 cm^{-1} and where the βC2-H7 and βC3-H8 modes in gas phase are predicted in different regions than the corresponding in aqueous solution. On the other hand, the out-of-plane deformation modes are predicted with A'' symmetries between 988 to 821 cm^{-1}. Hence, these modes can be assigned to the IR and Raman bands between 972 and 829 cm^{-1}.

4.5.1.2. BF_3 modes. As in similar salts, two anti-symmetrical (ν_a) and one symmetrical (ν_s) stretching modes are expected for the BF_3 group together with three deformation modes, two anti-symmetrical (δ_a) and one symmetrical (δ_s) modes, two rocking (ρ) and one twisting (τ_w) modes [1-5,7]. In this salt, ν_a and ν_s are predicted in different regions, thus, in gas phase ν_a is predicted at 1109 cm^{-1} while in solution at 991 cm^{-1} while ν_s is predicted at 853 and 849 cm^{-1} in gas phase and in solution, respectively. Here, it is evident the shifting of these modes due to the hydration of group. On the other hand, one ρ mode is predicted with A' symmetry while the other one with A'' symmetry between 219 and 210 cm^{-1}, hence, only these latter modes are assigned to the Raman band of medium intensity at 209 cm^{-1}. The τ_w modes were predicted at 18 and 29 cm^{-1} in gas phase and solution, hence, they cannot be assigned because bands in this region were not experimentally observed.

4.5.1.3. Skeletal modes. The C=O stretching mode is characteristic of trifluoroborate salts previously studied by our investigation group and, in FBTFB, the SQM calculations predicted these modes in both media with A' symmetry at 1544 cm^{-1} in gas phase and at 1595 cm^{-1} in solution. The hydration of this mode is simply seen by its slight shifting of position in gas phase toward higher wavenumbers in solution. These modes in FTFB and IFTB are predicted at 1582/1556 and 1621/1572 cm^{-1}, respectively while in HTFB and PTFB at 1673/1592 and 1620/1582 cm^{-1}, respectively [1-5,7]. These differences in the assignments of C=O stretching mode in the different salts clearly reveal that the position of this vibration mode is strongly dependent on the group or ring linked to C-C-BF_3-K moiety. Besides, we observed that the C-C and C-B stretching modes associated to the C-C-BF_3-K moiety are also dependent of medium because in solution those two modes are predicted by calculations at lower wavenumbers (1217 and 1179 cm^{-1}) than the values in gas phase (1229 and 1201 cm^{-1}). Evidently, the hydrations on the C=O and BF_3 groups belonging to C-C-BF_3-K moiety also have an effect on the two C-C and C-B stretching modes, as suggested by their shifting in solution. The expected $K18^+F16^-$ and $K18^+F17^-$ stretching modes were predicted by calculations in the lower wavenumbers region and with different A' and A'' symmetries in gas phase while in solution the two vibration modes were predicted with the same symmetry. Probably, this difference can be attributed to that one of the two ν_aBF_3 anti-symmetric modes is predicted with A'' symmetry in gas phase. Both K^+F^- stretching modes were not assigned because there is not Raman bands experimentally observed in that region. In addition, Table 4 shows clearly the assignments for other expected skeletal modes of this salt with different A' and A'' symmetries as, for example the deformation ring modes are visibly predicted with A' symmetries in both media while the corresponding torsions modes are predicted with A'' symmetries.

5. Force Fields

In the studies previous performed on these trifluoroborate salts, the force constants were calculated to characterize the different bonds, as predicted by AIM analyses. According to section computational details [1-7], these parameters were computed employing the SQMFF methodology and the Molvib program [13-15]. Hence, the main scaled internal force constants for FBTFB in gas and aqueous solution phases are compared with the corresponding to 2-phenylacetyl-trifluoroborate (PTFB) by using the functional hybrid B3LYP with the 6-311++G** basis set in **Table 5**. Analyzing, the force constants for FBTFB in both media it is observed that the *f(νC=O)* and *f(δBF$_3$)* force constants present slight variations in solution, as compared with the values in gas phase, in agreement with the differences observed in the corresponding C=O and BF_3 stretching modes analysed in the above section. Hence, the hydrations of those two groups are clearly supported by those two force constants. In the remaining constants practically are not observed changes in solution. If now the force constants for FBTFB are compared with the corresponding to PTFB in both media by using the same functional hybrid and basis set, we observed that all values are completely different due, naturally, to the structural differences between both salts. The presence of F atom in the phenyl ring of FBTFB and the existence of CH_2 group between the phenyl group and the C-C-BF_3-K moiety in PTFB perfectly justifies the differences in the force constants values of both salts. Very important results are the low *f(νC=O)* force constants values in gas phase and solution for FBTFB of 9.83 and 9.54 mdyn Å^{-1}, respectively as compared with the computed for PTFB (10.40 and 10.10 mdyn Å^{-1}). Here, the influence of F atom on phenyl ring is clearly observed in the enlargement of C=O bond and in the diminishing of its force constant, especially in solution.

6. Electronic spectrum

The experimental ultraviolet-visible spectrum of FBTFB in aqueous solution, recorded in the 182-400 nm region, is shown in **Figure 9** compared with the predicted spectra for the salts and its anion in the same medium by using TD-DFT calculations and the functional hybrid B3LYP with the 6-311++G** basis set. The positions of observed and calculated bands can be seen in **Table 6** together with the corresponding assignments. As observed in other salts [1-5,7], two bands and a shoulder are observed in the experimental spectrum, one intense band at 195.6 nm and other of medium intensity at c.a. 254.2 nm while the shoulder is observed at c.a. 242 nm. In the spectrum of salts four bands are clearly observed, two very strong, other with medium intensity and the other one weak, as was also observed in the anion but in different positions. The bands between 134.4 and 195.7 nm can be simply assigned to $n \rightarrow n^*$ transitions from the lone pairs of F atoms belong to BF_3 groups toward different anti-bonding lone pairs of B atom orbitals, as supported by the high energy values of

*LPF17→ LP*B14* transitions and, as revealed by NBO studies. On the other hand, the experimental band at 254.2 nm is assigned to $\pi \rightarrow \pi^*$ transitions due to the C=C bonds of phenyl ring, as observed in similar salts [1-5,7].

7 Conclusions

Potassium 1-fluorobenzoyltrifluoroborate (FBTFB) salt was characterized using Fourier Transformed Infrared (FT-IR) and Raman solid-state spectroscopies as well as ultraviolet-visible spectroscopy in aqueous solution. The functional hybrid B3LYP with the 6-311++G** basis set have optimized the structures of salt in gas phase and in aqueous solution with C_S symmetries. In solution, the influence of solvent was studied at the same level of theory with the integral equation formalism variant polarised continuum method (IEFPCM) and the universal solvation model. The FBTFB salt has evidenced the lower solvation energy (-81.54 kJ/mol), as compared with other trifluoroborate salts probably due to the presence of F in the 4th position of phenyl ring that decreases the solubility of this salt. NBO studies clearly support the ionic characteristics of K^+F^- and K^+O^- bonds and the high energy values of *LPF17→ LP*B14* transitions ($\Delta E_{n\rightarrow n^*}$) while the AIM analyses suggest a high stability of salt in both media due to three ionic and one C-H···F interactions. Analyses of frontier orbitals have suggested that the FBTFB salt is more reactive in solution than in gas phase and, than PTFB in the two media possibly because FBTFB presents higher global electrophilicity (ω) and nucleophilicity indexes (E) in both media than PTFB.

In this work, the salt was vibrationally characterized for the first time by using the calculated harmonic force fields, scaled force constants and complete assignments of all vibration normal modes expected for FBTFB in both media.

Acknowledgements. This work was supported with grants from CIUNT Project Nº 26/D608 (Consejo de Investigaciones, Universidad Nacional de Tucumán, Argentina). P. Leyton acknowledges to the project FONDEQUIP EQM130170 from CONICYT. E. Imbarack acknowledges the financial supports from Beca Doctorado Nacional Nº21140360 CONICYT. The authors would like to thank Prof. Tom Sundius for his permission to use MOLVIB.

Supporting Information Available: Tables S1-S6 and **Figures S1-S5**.

References

[1] M.A. Iramain, L. Davies, S.A. Brandán, FTIR, FT-Raman and UV-visible spectra of Potassium 3-furoyltrifluoroborate, J. Mol. Struct 1158 (2018) 245-254.

[2] M.A. Iramain, L. Davies, S.A. Brandán, Evaluating structures, properties and vibrational and electronic spectra of the potassium 2-isonicotinoyltrifluoroborate salt, J. Mol. Struct. 1163 (2018) 41-53.

[3] M.A. Iramain, L. Davies, S.A. Brandán, Structural and spectroscopic differences among the potassium 5-hydroxypentanoyltrifluoroborate salt and the furoyl and isonicotinoyl salts, J. Mol. Struct. 1176 (2019) 718-728.

[4] M.A. Iramain, A.E. Ledesma, S.A. Brandán, Structural properties and vibrational analysis of Potassium 5-Br-2-isonicotinoyltrifluoroborate salt. Effect of Br on the isonicotinoyl ring, J Mol. Struct. 1184 (2019) 146-156.

[5] M.A. Iramain, S.A. Brandán, Impact of Br on the isonicotinoyl ring and its effects on the properties of Potassium 5-Br-2-isonicotinoyltrifluoroborate salt in different media, submitted to J. Molecular Modeling (2019). In Press.

[6] M.A. Iramain, S.A. Brandán, Role of Halogen H···F Bonds in Potassium Trifluoroborate Salts, submitted to IJCAR, International Journal of Current Advanced Research 8(6A) (2019) 19248-19253.

[7] M.A. Iramain, E. Imbarack, P. Leyton Bongiorno, S.A. Brandán, Characterization of Potassium (2-phenylacetyl) trifluoroborate Salt by using the UV-Visible, FT-IR and FT-Raman spectra, J Mol. Struct. 1200 (2020) 127057.

[8] A.D. Becke, Density functional thermochemistry. III. The role of exact exchange, J. Chem. Phys. 98 (1993) 5648–5652.

[9] C. Lee, W. Yang, R.G. Parr, Development of the Colle-Salvetti correlation-energy formula into a functional of the electron density, Phys. Rev. B 37 (1988) 785–789.

[10] S. Miertus, E. Scrocco, J. Tomasi, Electrostatic interaction of a solute with a continuum. *Chem. Phys. 55 (1981) 117–*129.

[11] J. Tomasi, J. Persico, Molecular Interactions in Solution: An Overview of Methods Based on Continous Distributions of the Solvent, Chem. Rev. 94 (1994) 2027-2094.

[12] A.V. Marenich, C.J. Cramer, D.G. Truhlar, Universal solvation model based on solute electron density and a continuum model of the solvent defined by the bulk dielectric constant and atomic surface tensions, J. Phys. Chem. B113 (2009) 6378-6396.

[13] P. Pulay, G. Fogarasi, G. Pongor, J.E. Boggs, A. Vargha, Combination of theoretical ab initio and experimental information to obtain reliable harmonic force constants. Scaled quantum mechanical (QM) force fields for glyoxal, acrolein, butadiene, formaldehyde, and ethylene. J. Am. Chem. Soc., 105 (1983) 7073.

[14] T. Sundius, Scaling of ab-initio force fields by MOLVIB, Vib. Spectrosc. 29 (2002) 89-95.

[15] a) G. Rauhut, P. Pulay, Transferable scaling factors for density functional derived vibrational force fields. J. Phys. Chem. 99 (1995) 3093-3099. b) G. Rauhut, P. Pulay, J. Phys. Chem. 99 (1995) 14572.

[16] Gaussian 09, Revision A.02, M. J. Frisch, G. W. Trucks, H. B. Schlegel, G. E. Scuseria, M. A. Robb, J. R. Cheeseman, G. Scalmani, V. Barone, B. Mennucci, G. A. Petersson, H. Nakatsuji, M. Caricato, X. Li, H. P. Hratchian, A. F. Izmaylov, J. Bloino, G. Zheng, J. L. Sonnenberg, M. Hada, M. Ehara, K. Toyota, R. Fukuda, J. Hasegawa, M. Ishida, T. Nakajima, Y. Honda, O. Kitao, H. Nakai, T. Vreven, J. A. Montgomery, Jr., J. E. Peralta, F. Ogliaro, M. Bearpark, J. J. Heyd, E. Brothers, K. N. Kudin, V. N. Staroverov, R. Kobayashi, J. Normand, K. Raghavachari, A. Rendell, J. C. Burant, S. S. Iyengar, J. Tomasi, M. Cossi, N. Rega, J. M. Millam, M. Klene, J. E. Knox, J. B. Cross, V. Bakken, C. Adamo, J. Jaramillo, R. Gomperts, R. E. Stratmann, O. Yazyev, A. J. Austin, R. Cammi, C. Pomelli, J. W. Ochterski, R. L. Martin, K. Morokuma, V. G. Zakrzewski, G. A. Voth, P. Salvador, J. J. Dannenberg, S. Dapprich, A. D. Daniels, Ö. Farkas, J. B. Foresman, J. V. Ortiz, J. Cioslowski, and D. J. Fox, Gaussian, Inc., Wallingford CT, 2009.

[19] E.D. Gledening, J.K. Badenhoop, A.D. Reed, J.E. Carpenter, F.F. Weinhold, NBO 3.1; Theoretical Chemistry Institute, University of Wisconsin; Madison, WI, 1996**.**

[20] R. F.W. Bader, Atoms in Molecules. A Quantum Theory, Oxford University Press, Oxford, ISBN: 0198558651, 1990.

[21] F. Biegler-Köning, J. Schönbohm, D. Bayles, AIM2000; A Program to Analyze and Visualize Atoms in Molecules, J. Comput. Chem. 2001, 22, 545.

[22] A.B. Nielsen, A.J. Holder, *GaussView*, User´s Reference, GAUSSIAN, Inc.: Pittsburgh, PA, USA, 2000-2003.

[23] S.F. Boys, F. Bernardi, The calculation of small molecular interactions by the differences of separate total energies. Some procedures with reduced errors, Mol. Phys. 19 (1973) 553-566.

[24] R.G. Parr, R.G. Pearson, Absolute hardness: companion parameter to absolute electronegativity, J. Am. Chem. Soc. 105 (1983) 7512-7516.

[25] D. Romani, S.A. Brandán, M.J. Márquez, M.B. Márquez, Structural, topological and vibrational properties of an isothiazole derivatives series with antiviral activities, J. Mol. Struct. 1100 (2015) 279-289.

[26] D. Romani, S. Tsuchiya, M. Yotsu-Yamashita, S.A. Brandán, Spectroscopic and structural investigation on intermediates species structurally associated to the tricyclic bisguanidine compound and to the toxic agent, saxitoxin, J Mol. Struct. 1119 (2016) 25-38.

[27] E. Romano, L. Davies, S.A. Brandán, Structural properties and FTIR-Raman spectra of the anti-hypertensive, clonidine hydrochloride agent and their dimeric species, J Mol. Struct. 1133 (2017) 226-235.

[28] J. Kausteklis, V. Aleksa, M.A. Iramain, S.A. Brandán, Cation-anion interactions in 1-buthyl-3-methyl imidazolium nitrate ionic liquid and their effect on their structural and vibrational properties, J Mol. Struct. 1164 (2018) 1-14.

[29] J. Kausteklis, V. Aleksa, M.A. Iramain, S.A. Brandán, DFT study and vibrational assignment of 1-Butyl-3-methylimidazolium trifluoromethanesulfonate ionic liquid by using the FT-Raman spectrum, J Mol. Struct. 1175 (2019) 663-676.

[30] R.A. Rudyk, M.A. Checa, C.A.N. Catalán, S.A. Brandán, Structural, FT-IR, FT-Raman and ECD studies on the free base, cationic and hydrobromide species of scopolamine alkaloid, J Mol. Struct. 1180 (2019) 603-617.

[31] M.E. Manzur, S.A. Brandán, S(-) and R(+) Species Derived from Antihistaminic Promethazine Agent: Structural and Vibrational Studies, Heliyon 5 (2019) e02322.

[32] M.A. Iramain, M.V. Castillo, L. Davies, M.E. Manzur, S.A. Brandán, Structural and SQMFF study of potent insecticide 4′,4′-DDT Combining the FT-IR and FT-Raman spectra with DFT calculations, J Mol. Struct. 1199 (2020) 126964.

[33] P. Ugliengo, MOLDRAW Program, University of Torino, Dipartimento Chimica IFM, Torino, Italy, 1998.

[34] A.M. Dumas, J.W. Bode, Synthesis of acyltrifluoroborates, Org. Lett. *(*2012) 14(8) 2138-2141.

[35] E. Arunan, G.R. Desiraju, R.A. Klein, J. Sadlej, S. Scheiner, I. Alkorta, D.C. Clary, R.H. Crabtree, J.J. Dannenberg, Definition of the hydrogen bond (IUPAC Recommendations 2011, Pure and Applied Chemistry. 83(8) (2011) 1637–1641.

[36] G. Keresztury, S. Holly, G. Besenyei, J. Varga, A.Y. Wang, J.R. Durig, Vibrational spectra of monothiocarbamates-II. IR and Raman spectra, vibrational assignment, conformational analysis and *ab initio* calculations of *S*-methyl-*N,N*-dimethylthiocarbamate. Spectrochim. Acta, 49A (1993) 2007-2026.

Caption to Figures

Figure 1. Potential energy surfaces (PES) for the potassium 1-fluorobenzoyltrifluoroborate (FBTFB) salt described by the dihedral C3-C4-C12-B14 angle by using the B3LYP/6-311++G** method.

Figure 2. Molecular structure of the potassium 1-fluorobenzoyltrifluoroborate (FBTFB) salt and atom numbering.

Figure 3. Molecular structures of dimer and anionic species of the potassium 1-fluorobenzoyltrifluoroborate (FBTFB) salt and atom numbering.

Figure 4. Variations of volume (a) and dipole moment values (b) for the potassium 3-furoyl-trifluoroborate (FTFB), 2-isonicotinoyl-trifluoroborate (ITFB), 6-chloro-2-isonicotinoyl-trifluoroborate (Cl-ITFB), 4-fluorobenzoyl-trifluoroborate (FBTFB), 5-hydroxypentanoyl-trifluoroborate (HTFB), 5-Br-2-isonicotinoyl-trifluoroborate (Br-ITFB) and 2-phenylacetyl-trifluoroborate (PTFB) salts as function of molecular weights.

Figure 5. Molecular graphics of the 1-fluorobenzoyl-trifluoroborate (FBTFB) salt in gas phase showing the geometry of all their bond critical points (BCPs) and ring critical points (RCPs) at the B3LYP/6-311++G** level of theory.

Figure 6. Experimental FT-IR spectrum of the 1-fluorobenzoyl-trifluoroborate (FBTFB) salt in the solid state compared with the corresponding predicted for the monomer and its dimer by using B3LYP/6-311++G** level of theory.

Figure 7. Experimental Raman spectrum of the 1-fluorobenzoyl-trifluoroborate (FBTFB) salt in the solid state compared with the corresponding predicted for the monomer and its dimer by using B3LYP/6-311++G** level of theory.

Figure 8. Experimental Raman spectrum of the 1-fluorobenzoyl-trifluoroborate (FBTFB) salt in the solid state in the 2000-180 cm^{-1} region compared with the corresponding predicted for the monomer and its dimer by using B3LYP/6-311++G** level of theory.

Figure 9. Experimental Ultraviolet-visible spectrum in aqueous solution of the 1-fluorobenzoyl-trifluoroborate (FBTFB) salt compared with the corresponding predicted for the monomer and its anion by using B3LYP/6-311++G** level of theory.

Table 1. Total corrected by ZPVE Energy (E), moment dipolar (μ), volume (V) and solvation energy (ΔG) of potassium 1-fluorobenzoyl-trifluoroborate (FBTFB), in gas phase and aqueous solution by using the functional hybrid B3LYP and the 6-311++G** basis set.

B3LYP/6-311++G**				
Property	Gas phase	Aqueous solution	ΔE(kJ/mol)	ΔV(Å^3)
E (Hartrees) ZPVE	-1368.9232	-1368.9460	-59.80	
μ(D)	8.55	9.93		
V(Å^3)	250.7	253.3		2.3
Solvation energy (kJ/mol)				
Basis set	$\Delta G_u^{\#}$	ΔG_{ne}	ΔG_c	
6-311++G**	-59.80	21.74	-81.54	

Table 2. Total corrected by ZPVE Energy (E), moment dipolar (μ), volume (V) and solvation energy (ΔG) of potassium 1-fluorobenzoyl-trifluoroborate (FBTFB), in gas phase and aqueous solution by using the functional hybrid B3LYP and the 6-311++G** basis set.

Potassium trifluoroborate salts[a]									
B3LYP/6-311++G** Method									
Salts	MW (g/mol)	Gas phase			Aqueous solution				
		Volumen ($Å^3$)	μ (D)	Gap (eV)	Volumen ($Å^3$)	μ (D)	Gap (eV)	ΔV ($Å^3$)	ΔG_c (kJ/mol)
FTFB[b]	201.8	229.0	7.79	5.05	230.7	9.20	5.00	1.7	-85.65
HTFB[c]	207.8	252.9	8.40	4.99	255.7	10.19	5.56	2.8	-108.98
ITFB[d]	212.8	240.1	5.56	4.39	243.0	6.89	4.42	2.9	-94.58
PTFB[e]	225.8	259.2	7.98	4.81	261.6	9.42	5.16	2.4	-87.35
FBTFB[f]	229.8	250.7	8.54	4.69	253.3	9.93	4.65	2.3	-81.54
Cl-ITFB[g]	247.3	260.5	5.64	4.32	261.4	5.23	4.53	0.9	-93.03
Br-ITFB[h]	291.7	248.0	6.89	4.30	248.4	7.23	4.47	0.4	-88.81

[a]This work, [b]From Ref [1], [c]From Ref [3],[d]From Ref [2], [e]From Ref [7], [f]From Ref [6], [g]From Ref [6], [h]From Ref [4]

Table 3. Calculated geometrical parameters for the Potassium 1-fluorobenzoyl-trifluoroborate (FBTFB) in gas phase and aqueous solution by using the functional hybrid B3LYP and the 6-311++G** basis set.

	B3LYP/Method[a]		
Parameters	Gas phase	Aqueous solution	Exp[b]
	Bond lengths		
C1-C2	1.385	1.383	1.381
C2-C3	1.392	1.391	1.387
C3-C4	1.403	1.404	1.394
C4-C5	1.405	1.407	1.392
C5-C6	1.386	1.386	1.379
C1-F11	1.353	1.359	
C2-H7	1.082	1.082	0.959
C3-H8	1.081	1.080	0.975
C4-C12	1.489	1.485	1.492
C5-H9	1.083	1.082	0.954
C6-H10	1.083	1.083	0.938
C12-O13	1.245	1.246	1.239
C12-B14	1.657	1.649	1.636
B14-F15	1.381	1.400	1.409
B14-F16	1.447	1.440	1.410
B14-F17	1.447	1.440	1.425
K18-O13	2.598	2.691	
K18-B14	2.985	3.115	
K18-F16	2.575	2.707	2.690
K18-F17	2.575	2.707	
RMSD	**0.065**	**0.064**	
	Bond angles		
C1-C2-C3	118.4	118.1	118.4
C2-C3-C4	120.6	120.8	120.9
C3-C4-C5	118.9	118.8	118.9
C4-C5-C6	121.0	121.0	120.9
C5-C6-C1	118.2	118.0	118.8
C6-C1-C2	122.6	123.1	121.8
F11-C1-C2	118.8	118.5	
F11-C1-C6	118.4	118.3	
H7-C2-C3	121.6	121.5	119.6
H7-C2-C1	119.8	120.3	121.7
H8-C3-C4	119.5	120.0	121.8
H8-C3-C2	119.8	119.0	117.2
C12-C4-C5	119.4	119.7	120.5
C12-C4-C3	121.6	121.4	120.4
H9-C5-C6	120.5	119.5	120.1
H9-C5-C4	118.4	119.4	118.9
H10-C6-C1	119.6	120.1	120.8
H10-C6-C5	122.0	121.8	120.3
C4-C12-O13	118.1	118.9	119.2
O13-C12-B14	115.3	114.2	119.7
C12-B14-F15	118.1	118.6	112.9
C12-B14-F16	106.1	107.1	111.4
C12-B14-F17	106.1	107.1	111.3
B14-F16-K18	91.4	92.2	
B14-F17-K18	91.4	92.2	
C12-O13-K18	109.6	112.6	
F16-K18-F17	52.8	50.1	
O13-K18-F16	67.0	63.7	
O13-K18-F17	67.0	63.7	

RMSD	**1.0**	**1.0**	
	Dihedral angles		
C4-12-C13-K18	180.0	180.0	
C4-C12-B14-F15	0.0	0.0	-46.3
C4-C12-B14-F16	124.4	123.5	73.0
C4-C12-B14-F17	-124.4	-123.5	-167.2
C12-B14-F16-K18	71.6	72.6	120.6
C12-B14-F17-K18	-71.6	-72.6	
RMSD	**47.5**	**47.2**	

[a]This work, [b]From Ref [34]

Table 4. Observed and calculated wavenumbers (cm^{-1}) and assignments for Potassium 1-fluorobenzoyltrifluoroborate (FBTFB) in gas phase and in aqueous solution by using the functional hybrid B3LYP and the 6-311++G** basis set.

Experimental[a]			B3LYP 6-311++G**[a]							
			Gas				PCM			
Modes	IR	Raman	SQM[b]	Calc[c]	Inten[d].	Assignment[a]	SQM[b]	Calc[c]	Inten[d]	Assignment[a]
A' Symmetry										
1	3088vw		3092	3225.4	12,3	νC3-H8	3095	3228.8	10.3	νC3-H8
2	3066vw		3070	3202.9	5.7	νC5-H9	3072	3205	7.7	νC5-H9
3	3054vw		3066	3198.5	1.8	νC2-H7	3068	3200	2.6	νC2-H7
4	3043vw		3058	3189	0.6	νC6-H10	3061	3193.3	0.9	νC6-H10
5	1637vs	1643w	1594	1650.5	32.3	νC5-C6	1595	1652.3	111.8	νC12=O13
6	1587s	1585vw	1574	1627.4	95.2	νC6-C1	1570	1624.3	81.0	νC6-C1, νC3-C4
7	1530w		1544	1601.9	385.6	νC12=O13	1546	1602.8	557.4	νC1-C2
8			1481	1529.1	16.3	βC3-H8	1475	1522.6	35.4	βC3-H8
9	1408vw		1391	1437.5	27.3	νC2-C3	1386	1432.4	36.5	νC2-C3, νC5-C6
10	1300w	1305vw	1295	1342.2	24.3	νC3-C4	1291	1339.4	33.9	νC4-C5
11	1256m	1265m	1289	1326.9	2.7	νC1-C2	1286	1322.3	4.4	νC1-C2
12	1231w	1238w	1229	1268.2	162.8	νC4-C12	1217	1255.1	197.2	νC4-C12
13			1201	1242.1	92.8	νC1-F11	1179	1219.9	2.7	νC1-F11
14	1151w	1155m	1144	1177.4	79.0	βC2-H7	1138	1171.6	144.2	βC2-H7
15	1111w	1110m	1109	1137.8	205.8	ν_aBF_3	1085	1118.0	4.3	βC6-H10, βC5-H9
16	1089m	1070vw	1085	1118.1	34.2	βC6-H10, βC5-H9	1037	1063.1	289.6	νC12-B14
17	1018s	1014vw	1015	1034.8	160.7	βR_1	1004	1026.9	30.3	βR_1
18	1009s	1010vw	1003	1029.8	2.7	νC4-C5	991	1013.2	372.9	ν_aBF_3
19	895m		853	875.0	353.0	ν_sBF_3	849	869.3	497.5	ν_sBF_3
20	805w		798	819.5	15.1	βR_3	793	814.4	15.0	νC1-F11
21		637s	640	650.4	14.7	βR_2	638	647.7	10.4	βR_2
22			627	640.6	7.7	ν_sBF_3	624	638.5	7.0	βR_3
23			588	597.6	63.2	δ_sBF_3	584	592.8	114.5	δ_sBF_3
24			520	527.3	2.1	δB14C12C4	513	520.0	3.8	δB14C12C4
25		439m	435	440.1	6.3	δ_aBF_3	426	432.0	9.8	δ_aBF_3
26			397	404.5	3.6	βC1-F11	391	398.7	2.9	βC1-F11
27		364w	374	379.8	14.0	βC12=O13	357	361.8	10.9	βC12=O13
28		280w	249	255.0	6.9	νC12-B14	245	251.32	7.6	βC4-C12
29			237	240.0	7.9	ρBF_3	228	229.6	9.3	ρBF_3
30			190	197.1	42.3	νF16-K18	141	142.0	1.5	δB14C12C4
31			153	153.8	3.6	δK18B14C12	119	123.4	52.2	νF16-K18
32			98	99.0	14.8	βC4-C121	50	60.0	26.9	νF17-K18
A'' Symmetry										
33	972vs	964vw	988	998.2	0.6	γC6-H10	988	998.5	0.1	γC5-H9
34	952s	958vw	973	981.8	12.3	γC3-H8	971	979.1	17.5	γC3-H8
35		903s	902	919.3	256.7	ν_aBF_3	910	927.4	416.8	ν_aBF_3
36	840m	845m	849	860.1	6.6	γC2-H7	846	859.8	21.0	γC6-H10
37	829m	831w	824	835.0	0.1	γC5-H9	821	833.0	0.3	γC2-H7
38	732m	738vw	729	747.7	35.5	γC1-F11	728	746.3	53.0	τR_1
39	663w	663s	661	678.3	39.8	τR_1	660	676.8	62.8	γC12-O13
40		503w	504	514.0	9.2	τR_2	502	511.6	17.9	γC1-F11
41		408m	412	424.8	0.1	τR_3	414	425.1	0.1	δ_aBF_3
42		373w	405	409.9	1.2	δ_aBF_3	406	412.2	4.9	τR_3
43		309s	301	306.5	0.1	γC12-O13	300	305.5	0.1	γC12-O13
44		209m	219	227.9	0.9	$\rho'BF_3$	210	215.6	2.3	$\rho'BF_3$
45			119	125.0	12.9	νF17-K18	106	109.7	10.5	τR_2
46			109	112.1	0.1	τR_2	58	51.8	13.8	δK18B14C12
47			40	43.8	0.1	τwC4-C12, γC12-O13	43	33.5	0.6	τwC4-C12
48			18	25.5	5.0	τwBF_3	29	7.9	3.9	τwBF_3

Abbreviations: ν, stretching; δ, deformation in the plane; γ, deformation out of plane; wag, wagging; τ, torsion; β_R, deformation ring; τ_R, torsion ring; ρ, rocking; τ_w, twisting; δ, deformation; a, antisymmetric; s, symmetric; [a]This work, [b]From scaled quantum mechanics force field, [c]From B3LYP/6-311++G** calculation, [d]Units in $km.mol^{-1}$.

Table 5: Main scaled internal force constants for Potassium 1-fluorobenzoyl-trifluoroborate (FBTFB) in gas and aqueous solution phases compared with the corresponding to 2-phenylacetyl-trifluoroborate (PTFB) by using the functional hybrid B3LYP and the 6-311++G** basis set.

Force constants	B3LYP/6311++G**			
	Gas phase		Aqueous solution	
	FBTFB[a]	PTFB[b]	FBTFB[a]	PTFB[b]
$f(\nu C\text{-}H)_R$	5.18	5.14	5.20	5.12
$f(\nu C\text{-}C)_R$	6.36	5.99	6.35	6.00
$f(\nu C\text{-}B)$	2.83	2.90	2.90	2.90
$f(\nu BF_3)$	3.78	4.10	3.61	3.93
$f(\nu C{=}O)$	9.83	10.40	9.54	10.10
$f(\delta C\text{-}C\text{-}B)$	1.39	1.00	1.39	1.00
$f(\delta BF_3)$	1.26	1.40	1.22	1.37

Units are mdyn $Å^{-1}$ for stretching and mdyn Å rad^{-2} for angle deformations, [a]This work, [b]From Ref. [7]

Table 6. TD-DFT calculated visible absorption wavelengths (nm) for Potassium 1-fluorobenzoyl-trifluoroborate (FBTFB) in aqueous solution by using the functional hybrid B3LYP and the 6-311++G** basis set compared with the corresponding experimental for the anion in the same medium.

Experimental[a]	B3LYP/6-311++G**[a]		Assignment[a]
	Salt	Anion	
	142.5w	134.4w	n→n*
	167.9vs	168.7vs	n→n*
195.6vs	194.6vs	195.7vs	n→n*
242sh			
254.2m	255.7m	251.2m	π→π*(C=C)

[a]This work. Abbreviations: vs, very strong; m, medium; w, weak; sh, shoulder

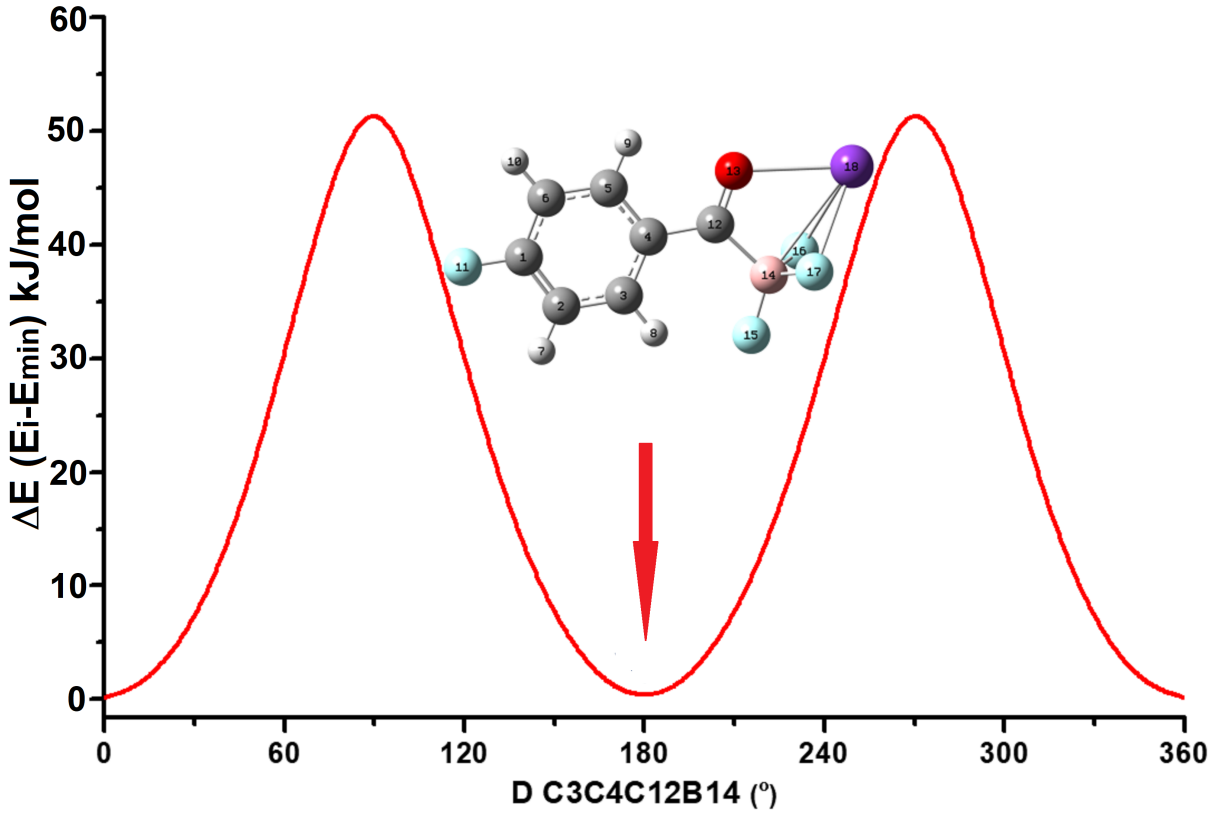
ΔE (Ei-Emin) kJ/mol
60
50
40
30
20
10
0
0
60
120
180
240
300
360
D C3C4C12B14 (°)

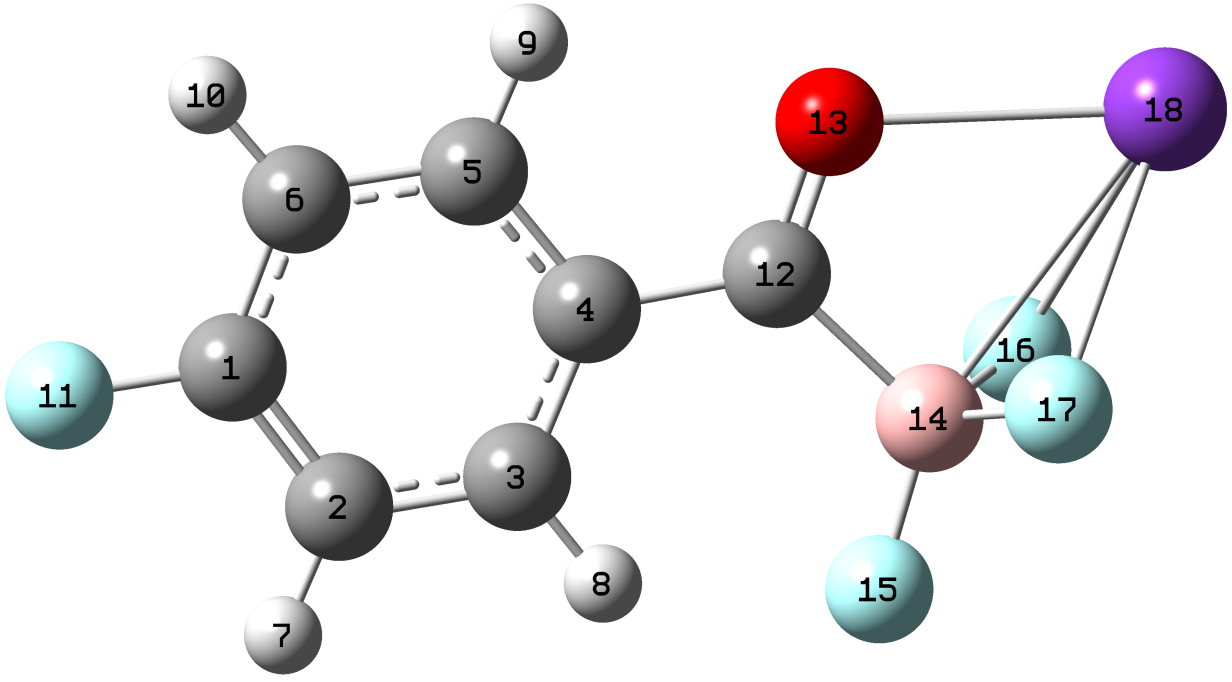

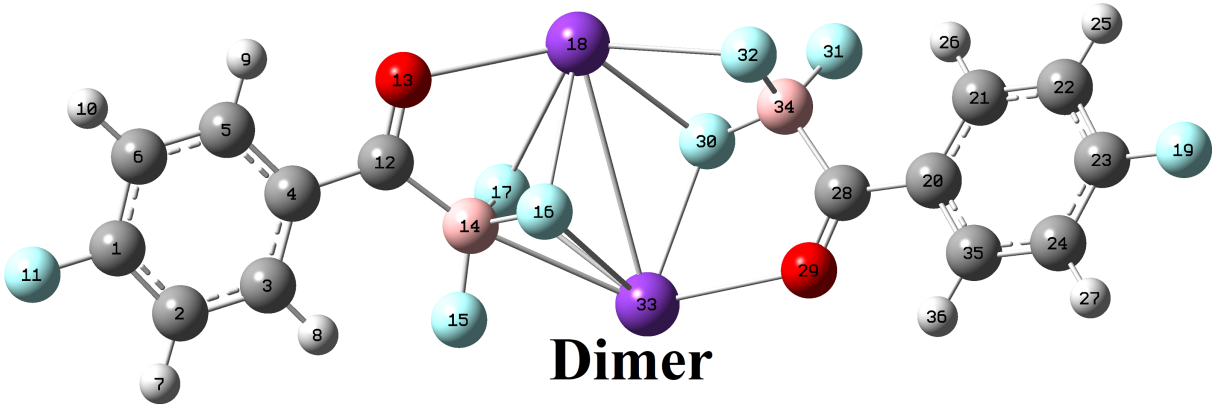

Dimer

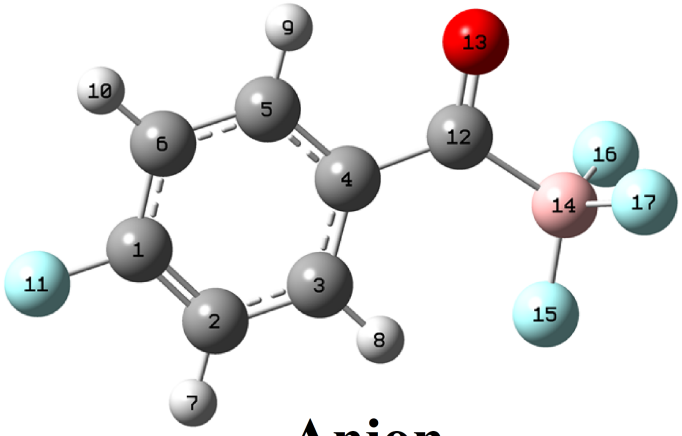

Anion

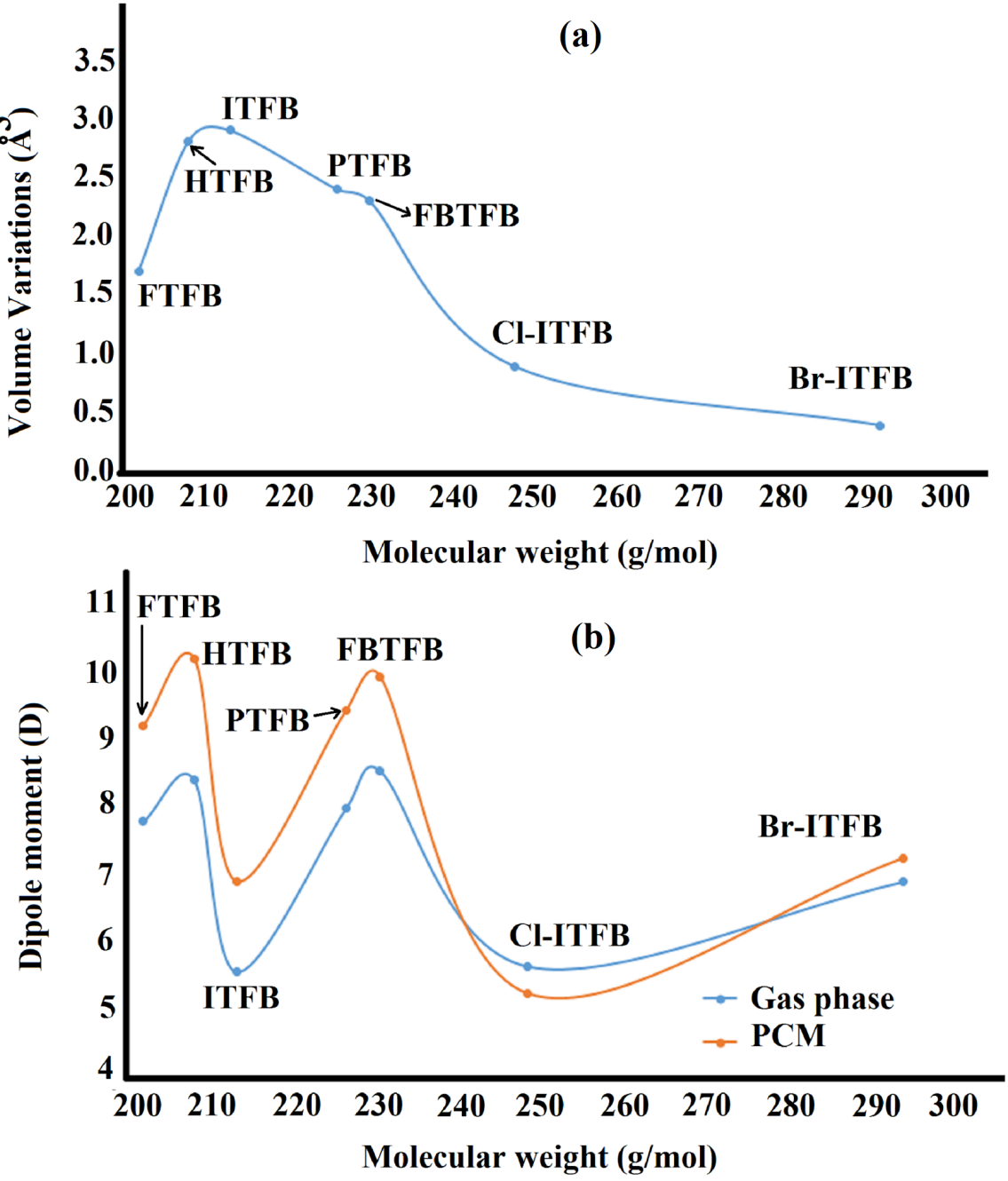
(a)
Volume Variations (Å3)
3.5
3.0
2.5
2.0
1.5
1.0
0.5
0.0
ITFB
HTFB
PTFB
FBTFB
FTFB
Cl-ITFB
Br-ITFB
200 210 220 230 240 250 260 270 280 290 300
Molecular weight (g/mol)
(b)
Dipole moment (D)
11
10
9
8
7
6
5
4
FTFB
HTFB
FBTFB
PTFB
Br-ITFB
Cl-ITFB
ITFB
Gas phase
PCM
200 210 220 230 240 250 260 270 280 290 300
Molecular weight (g/mol)

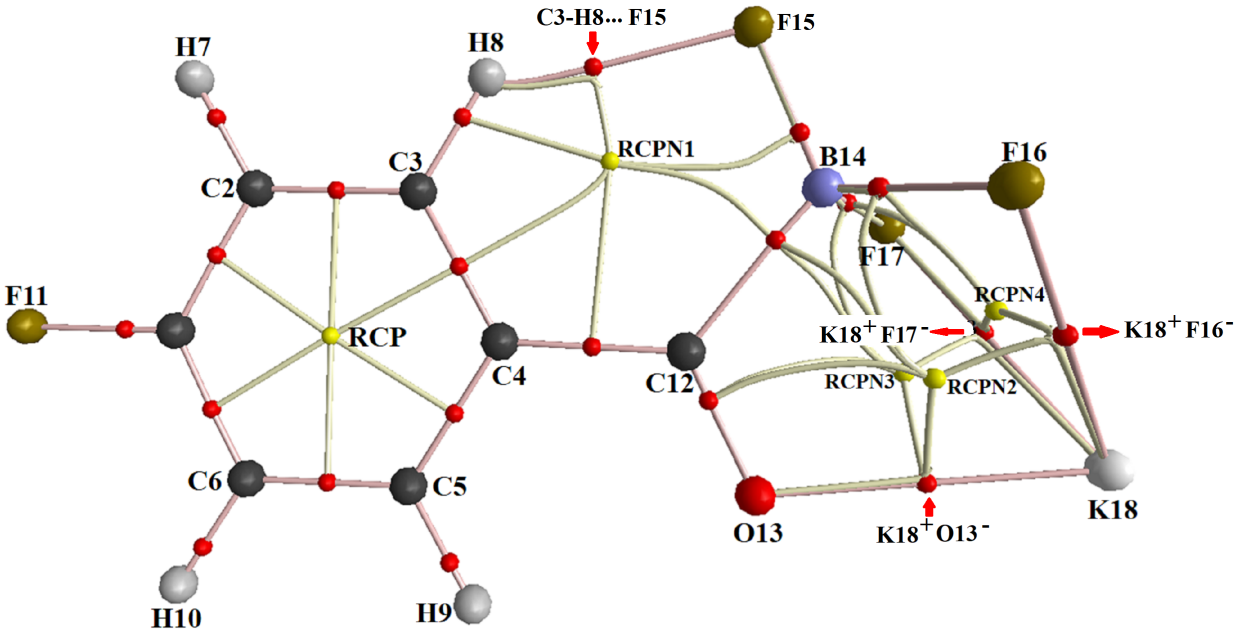

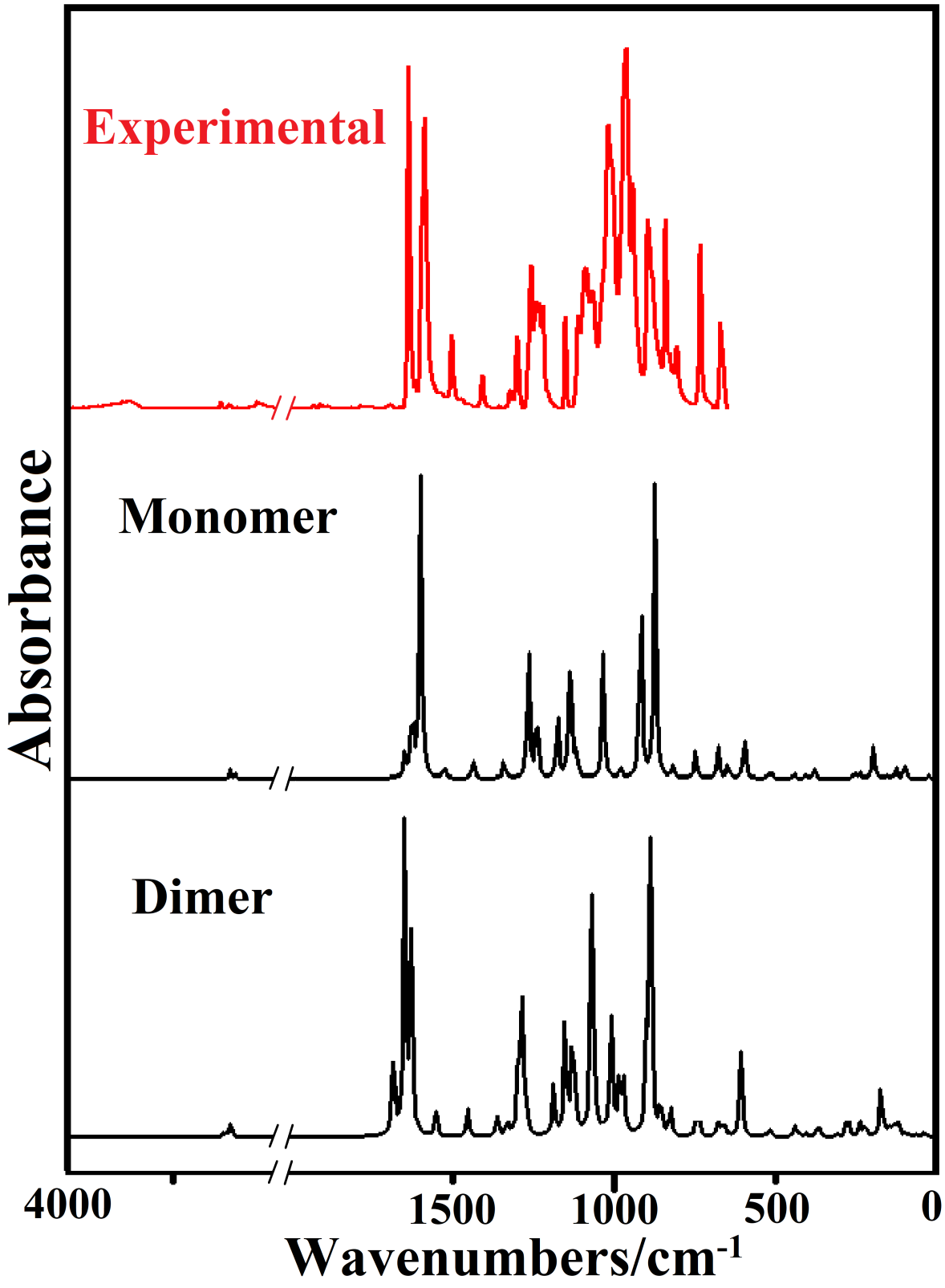
Experimental
Monomer
Dimer
Absorbance
4000
1500
1000
500
0
Wavenumbers/cm-1

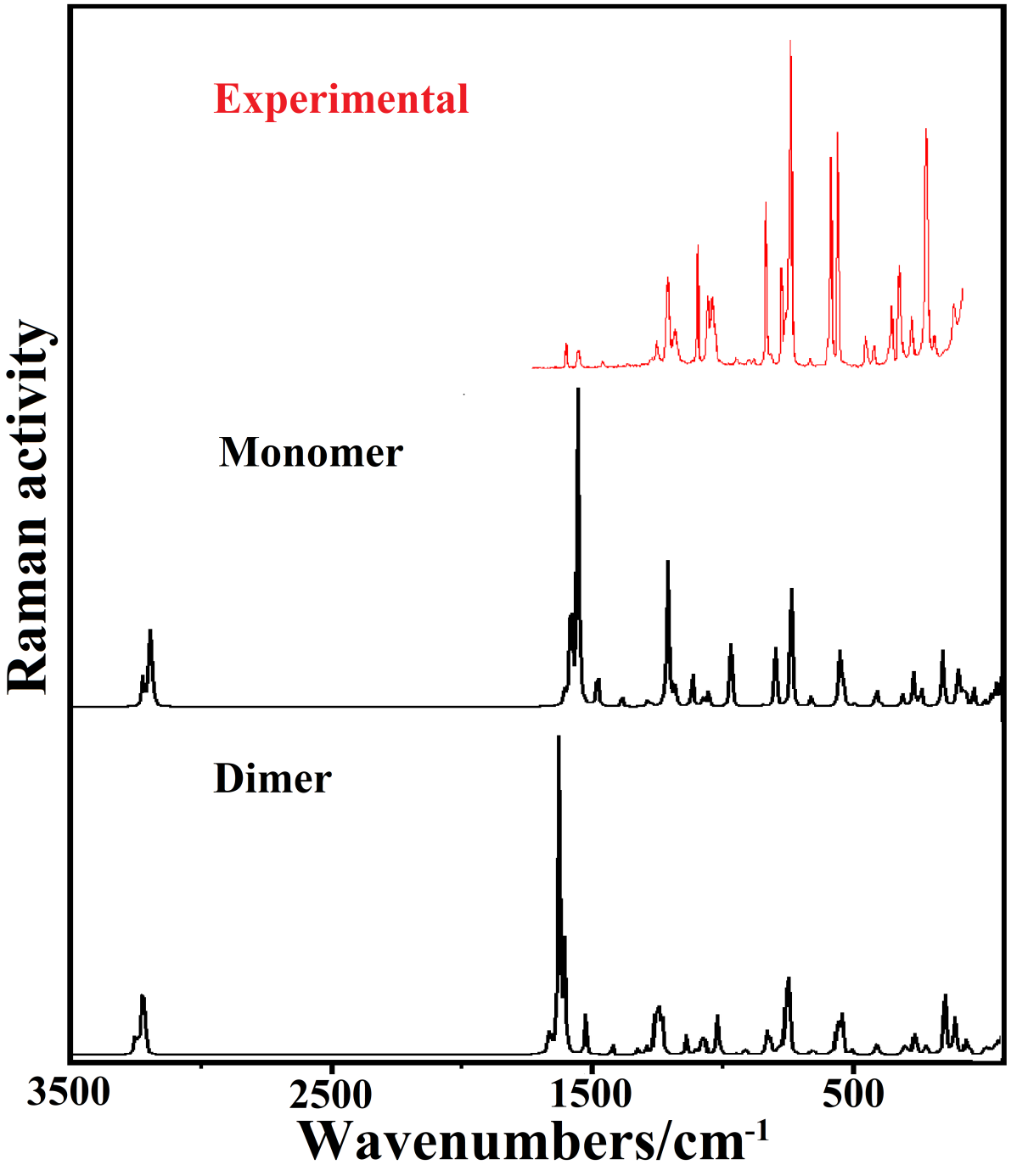
Experimental
Monomer
Dimer
Raman activity
3500
2500
1500
500
Wavenumbers/cm-1

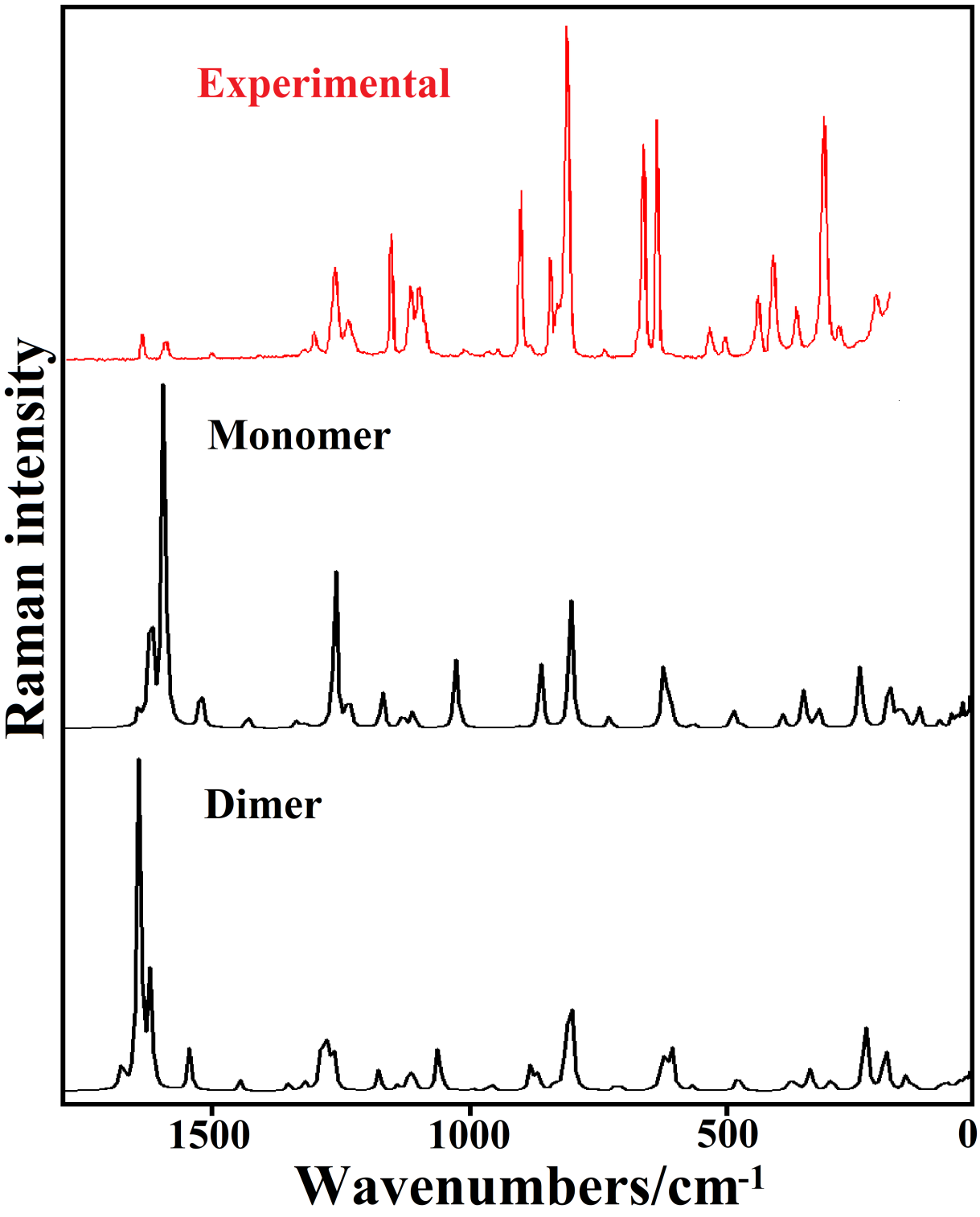
Experimental
Monomer
Dimer
Raman intensity
1500
1000
500
0
Wavenumbers/cm-1

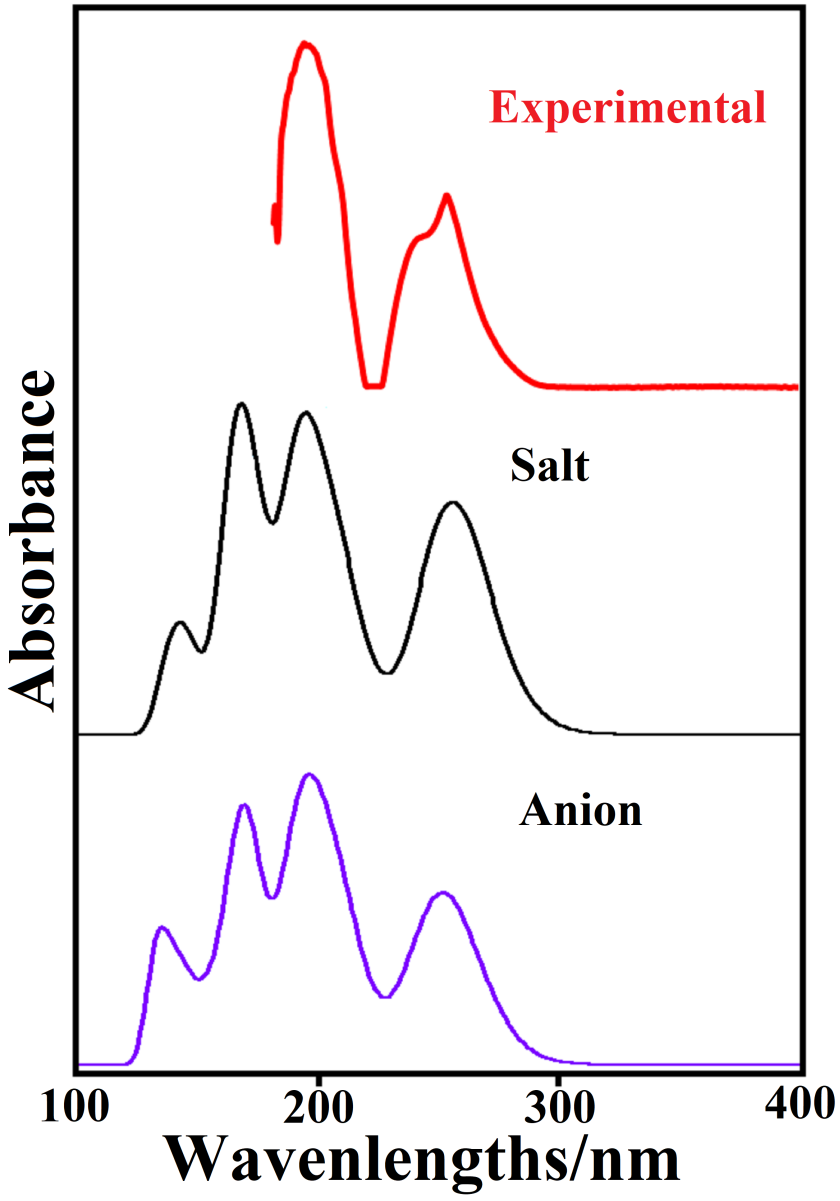
Experimental
Salt
Anion
Absorbance
100
200
300
400
Wavenlengths/nm

HIGHLIGHTS

FBTFB salt was characterized by the FT-IR, Raman and the UV-visible spectra

FBTFB has evidenced a low solvation energy as compared with similar salts

NBO studies support clearly the ionic characteristics of K^+F^- and K^+O^- bonds

AIM analyses suggest a high stability of salt in both media

FBTFB present high global electrophilicity and nucleophilicity indexes in both media

Authors contribution section

Maximiliano A. Iramain: Performed the experiments

Ana E. Ledesma: Performed Infrared spectrum

Elizabeth Imbarack: Performed Raman spectrum

Patricio Leyton Bongiorno: Contributed reagents, materials

Silvia A. Brandán: Conceived and designed the experiments; Performed the experiments; Analyzed and interpreted the data; analysis tools or data; Wrote the paper.

UNIVERSIDAD NACIONAL DE TUCUMAN
FACULTAD DE BIOQUIMICA QUIMICA Y FARMACIA
INSTITUTO DE QUÍMICA INORGÁNICA
CÁTEDRA DE QUÍMICA GENERAL
Ayacucho 471 – T. E. 0054 381-4247752 interno 7073 - FAX 0054 381- 4248169
T4000CAN – San Miguel de Tucumán – República Argentina

San Miguel de Tucumán, October, 16, 2019

DECLARATION OF INTEREST STATEMENT

Maximiliano A. Iramain: Performed the experiments

Ana E. Ledesma: Performed Infrared spectrum

Elizabeth Imbarack: Performed Raman spectrum

Patricio Leyton Bongiorno: Contributed reagents, materials

Silvia A. Brandán: Conceived and designed the experiments; Performed the experiments; Analyzed and interpreted the data; analysis tools or data; Wrote the paper.

The authors declare no conflict of interest.